Int. J. Solids Structures Vol. 29, No. 23, pp. 3011–3023, 1992
Printed in Great Britain.

0020–7683/92 $5.00 + .00

A SPATIALLY CURVED AND TWISTED ROD ELEMENT FOR BUCKLING ANALYSIS

B. TABARROK and Y. XIONG
Department of Mechanical Engineering, University of Victoria, Victoria, BC, Canada V8W 2Y2

(*Received* 2 *March* 1991; *in revised form* 20 *April* 1992)

Abstract—By considering perturbations about the critical state the governing equations for the buckling of spatial rods are derived. These equations involve the curvature and twist of the rod which in general are different from those of the initial, i.e. unloaded, geometry. An incremental procedure is outlined for updating the rod's geometry up to the critical state. Other generalities incorporated into the analysis include the effect of the initial bending moments and shear forces as well as the axial loads. Based on the theory outlined it is shown how an exact stiffness matrix and an approximate geometric stiffness matrix may be developed for a curved and twisted rod. Through several examples the theory is verified and the performance of the element developed is assessed.

1. INTRODUCTION

Spatially curved and twisted rods are used in many mechanical and aeronautical engineering systems. For purposes of linear stress analysis such rods are often modelled by an assemblage of prismatic beam elements. For buckling analysis however such a representation has a number of drawbacks. The most important of these is that in the standard linear buckling analysis of beam systems, initial deformations are ignored. This is acceptable for such systems as pretwisted rods and deep arches which exhibit insignificant changes in geometry before buckling. On the other hand for systems such as helices which under most loading conditions exhibit appreciable changes in geometry before buckling a linear buckling analysis will lead to erroneous results. Furthermore the conventional geometric stiffness matrix of prismatic beam elements used in commercial F.E. programs, takes account of initial *axial* loads only. Accordingly a representation by prismatic elements will overlook the effect of initial bending moments and shear forces. It should also be noted that the representation of curved and twisted rods by prismatic elements introduces an added error into the analysis; namely the geometric error. Reduction of this error requires the use of a large number of elements and results in large size system matrices. This increase in the size of the system matrices is generally not of major concern for linear stress analysis, governed by linear algebraic equations. However, for buckling analysis governed by eigenvalue equations, the increase in the size of system matrices is of importance from a computational perspective. Furthermore in the presence of geometric errors the bounds on the eigenvalues are lost.

Until recently, spatially curved and twisted rod elements had received little attention. However there is extensive literature on the elements for purely curved and purely pretwisted rods [see, e.g., Abbas (1979), Tomas and Dokumaci (1974), Yamada and Ezawa (1977) and Ye and Gallagher (1983)]. For curved *and* pretwisted rods of circular cross-section an exact stiffness matrix was derived by Mottershead (1980). Mottershead (1982) also derived a consistent mass matrix and through the addition of some inconsistent nonlinear terms in the strain–displacement relations he investigated the dynamic stability of helical springs. A constant strain curved and twisted element was derived by Tabarrok *et al.* (1988a) for static and Tabarrok *et al.* (1988b) for dynamic analysis of spatial rods. For buckling analysis Xiong and Tabarrok (1989) developed an approximate geometric stiffness matrix based on a simplified set of equilibrium equations which accounted for initial axial loads only.

In this study a more comprehensive analysis is carried out and element matrices are derived for the linear and nonlinear buckling behaviour of spatial rods. In addition to the initial axial load, the formulation takes into account the initial moments and shear forces

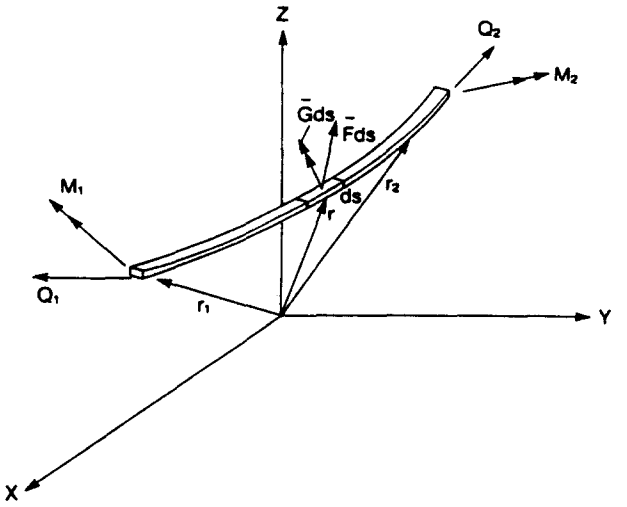

Fig. 1. Internal and applied forces.

as well as initial deformations. The latter is accomplished through the updating of the curvature and twist of the rod under increasing loads. The present element may be used for conservative and nonconservative buckling analysis of spatial rods. The performance of the element developed is assessed through the comparison of the results obtained, for several examples, with those given in the literature.

2. EQUILIBRIUM EQUATIONS

For small deformation linear analysis the equilibrium equations of spatial rods may be expressed as

$$\mathbf{Q}' + \mathbf{K}_0 \times \mathbf{Q} + \mathbf{F}_0 = 0, \tag{1}$$

$$\mathbf{M}' + \mathbf{K}_0 \times \mathbf{M} + \mathbf{t}_0 \times \mathbf{Q} + \mathbf{G}_0 = 0, \tag{2}$$

where $\mathbf{Q}$ denotes the vector of internal forces, $\mathbf{M}$ the vector of internal moments and $\mathbf{F}$ and $\mathbf{G}$ are vectors of external forces and moments, respectively (see Fig. 1). While $\mathbf{t}$ is the unit tangential vector to the centreline of the rod, $\mathbf{K}$ is the vector of curvature κ and torsion τ. The subscript 0 indicates the quantity in the initial (undeformed) state. Using the principal coordinate system as shown in Fig. 2, with $\mathbf{e}_1$ as the unit principal normal, $\mathbf{e}_2$ the unit binormal and $\mathbf{e}_3$, the unit tangent, one can write all vector quantities in component forms. For instance, the curvature vector and the unit tangential vector for the initial state may be expressed as

$$\mathbf{K}_0 = \kappa_0 \mathbf{e}_{02} + \tau_0 \mathbf{e}_{03}, \tag{3}$$

$$\mathbf{t}_0 = \mathbf{e}_{03}. \tag{4}$$

From eqn (3) and Fig. 2 it can be seen that the normal and the binormal directions of the rod's *centreline* are assumed to coincide with the principal directions of the rod's cross-section. Clearly this is the case for most curved and twisted rods used in practice, e.g. helical springs, but apart from the special case of the circular cross-section the two sets of directions need not be coincident.

By introducing the constitutive equations and strain-displacement relations one can describe the equilibrium equations in terms of displacements (u_1, u_2, u_3) and rotations $(\theta_1, \theta_2, \theta_3)$.

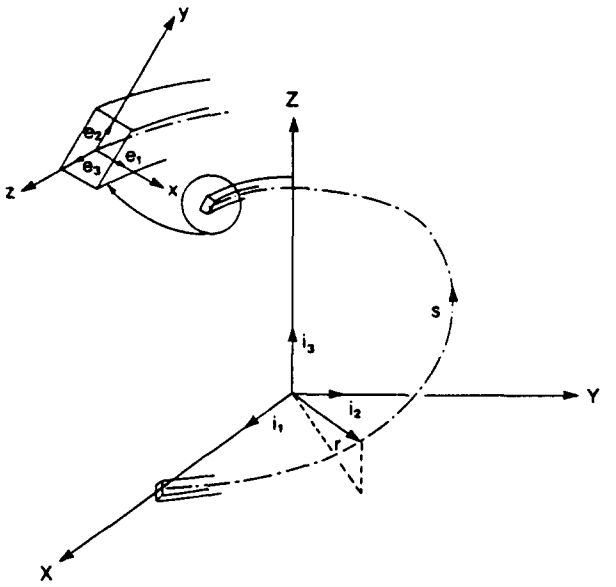

Fig. 2. Global and local frames.

Now along its axis a rod is generally quite stiff, but its flexibility in bending and torsion can give rise to significant changes in its original, i.e. unloaded, geometry. These changes in geometry are largely governed by finite rotations which bring about changes in **K** and **t**. One can show that for moderate rotations, these changes take the following forms for rods with uniform curvature and twist [see Tabarrok and Xiong (1989)]:

$$(\kappa-\kappa_0) = u_1'' - 2\tau_0 u_2' + \kappa_0 u_3' - \tau_0^2 u_1, \tag{5}$$

$$(\tau-\tau_0) = \theta_3' + \kappa_0 u_2' + \kappa_0\tau_0 u_1, \tag{6}$$

$$(\mathbf{e}_3-\mathbf{e}_{03}) = (u_1' - \tau_0 u_2 + \kappa_0 u_3)\mathbf{e}_{01} + (u_2' + \tau_0 u_1)\mathbf{e}_{02}. \tag{7}$$

Thus by applying the loads incrementally one can update the rod's geometry through the above equations and finally obtain the solution of the equilibrium equations in the deformed state. If one uses a convective set of coordinates, then the current coordinate system will remain as the principal axes of the cross-section, in which case

$$\mathbf{K} = \kappa\mathbf{e}_2 + \tau\mathbf{e}_3 \quad \text{and} \quad \mathbf{t} = \mathbf{e}_3. \tag{8}$$

3. PERTURBATION ABOUT THE CRITICAL STATE

Let us suppose that the deformed state is in the critical state, i.e. there exist other equilibrium states in the vicinity of this state. To examine these adjacent equilibrium states we consider a perturbation about the critical state. We denote the quantities in the perturbed state as follows:

$$\tilde{\mathbf{Q}} = \mathbf{Q}+\mathbf{q}, \quad \tilde{\mathbf{M}} = \mathbf{M}+\mathbf{m}, \quad \tilde{\mathbf{K}} = \mathbf{K}+\Delta\mathbf{K}, \tag{9}$$

$$\tilde{\mathbf{F}} = \mathbf{F}+\mathbf{f}, \quad \tilde{\mathbf{G}} = \mathbf{G}+\mathbf{g}. \tag{10}$$

These quantities will be referred to the *coordinate system in the critical state*. Since this coordinate system will not be along the principal axes of the cross-section in the perturbed state, there will arise a change of curvature in the principal normal direction, i.e.

$$\Delta\mathbf{K} = \kappa^*\mathbf{e}_2 + \tau^*\mathbf{e}_3 + \kappa_1^*\mathbf{e}_1. \tag{11}$$

Now since both the critical state and the perturbed state are possible equilibrium configurations, it follows that

$$\mathbf{Q}' + \mathbf{K}\times\mathbf{Q} + \mathbf{F} = \mathbf{0}, \tag{12}$$

$$\mathbf{M}' + \mathbf{K}\times\mathbf{M} + \mathbf{t}\times\mathbf{Q} + \mathbf{G} = \mathbf{0}, \tag{13}$$

and

$$(\mathbf{Q}+\mathbf{q})' + (\mathbf{K}+\Delta\mathbf{K})\times(\mathbf{Q}+\mathbf{q}) + \mathbf{F} = \mathbf{0}, \tag{14}$$

$$(\mathbf{M}+\mathbf{m})' + (\mathbf{K}+\Delta\mathbf{K})\times(\mathbf{M}+\mathbf{m}) + \mathbf{t}\times(\mathbf{Q}+\mathbf{q}) + \mathbf{G} = \mathbf{0}. \tag{15}$$

These equations apply to the conservative case, and the analysis of nonconservative loading is addressed in the appendix. Now neglecting quantities of second order of smallness and subtracting eqns (12) and (13) from (14) and (15) respectively, we find the governing equations for the perturbed quantities, expressed in component form, as follows:

$$q_1' - \tau q_2 + \kappa q_3 - \tau^* Q_2 + \kappa^* Q_3 = 0, \tag{16}$$

$$q_2' + \tau q_1 - \kappa_1^* Q_3 + \tau^* Q_1 = 0, \tag{17}$$

$$q_3' - \kappa q_1 - \kappa^* Q_1 + \kappa_1^* Q_2 = 0, \tag{18}$$

$$m_1' - \tau m_2 + \kappa m_3 - q_2 - \tau^* M_2 + \kappa^* M_3 = 0, \tag{19}$$

$$m_2' + \tau m_1 + q_1 - \kappa_1^* M_3 + \tau^* M_1 = 0, \tag{20}$$

$$m_3' - \kappa m_1 - \kappa^* M_1 + \kappa_1^* M_2 = 0. \tag{21}$$

The changes in the curvature vector may be expressed in terms of incremental displacements (u_1^*, u_2^*, u_3^*) and the axial rotation θ_3^*. These expressions are essentially similar to those in eqns (5) and (6) except that now there is an additional change of curvature; namely κ_1^*. These are given by Tabarrok and Xiong (1989):

$$\kappa^* = u_1^{*\prime\prime} - 2\tau u_2^{*\prime} + \kappa u_3^{*\prime} - \tau^2 u_1^*, \tag{22}$$

$$\tau^* = \theta_3^{*\prime} + \kappa u_2^{*\prime} + \kappa\tau u_1^*, \tag{23}$$

$$\kappa_1^* = -u_2^{*\prime\prime} - 2\tau u_1^{*\prime} + \tau^2 u_2^* - \tau\kappa u_3^* + \kappa\theta_3^*. \tag{24}$$

It now remains to introduce the constitutive and displacement strain relations. For a homogeneous and isotropic beam undergoing small strain, these equations are given by

$$\frac{q_1}{\gamma GA} = \varepsilon_1^* = u_1^{*\prime} - \tau u_2^* + \kappa u_3^* - \theta_2^*, \tag{25}$$

$$\frac{q_2}{\gamma GA} = \varepsilon_2^* = u_2^{*\prime} + \tau u_1^* + \theta_1^*, \tag{26}$$

$$\frac{q_3}{EA} = \varepsilon_3^* = u_3^{*\prime} - \kappa u_1^*, \tag{27}$$

$$\frac{m_1}{EI_1} = k_1^* = \theta_1^{*\prime} - \tau\theta_2^* + \kappa\theta_3^*, \tag{28}$$

$$\frac{m_2}{EI_2} = k_2^* = \theta_2^{*\prime} + \tau\theta_1^*, \tag{29}$$

$$\frac{m_3}{GI_3} = k_3^* = \theta_3^{*\prime} - \kappa\theta_1^*, \tag{30}$$

where

γ = shear coefficient,
E = Young's modulus,
G = shear modulus,
A = area of cross-section,
I_1, I_2 = second moments of area,
I_3 = torsional constant,
k_1^*, k_2^*, k_3^* = incremental curvature quantities associated with m_1, m_2, m_3,
$\varepsilon_1^*, \varepsilon_2^*, \varepsilon_3^*$ = incremental strain quantities associated with q_1, q_2, q_3.

By suppressing the shear strains in eqns (25), (26) and using the resulting constraint equations in eqns (28)–(30) one can readily recover the changes in curvature and twist of the centreline as given in eqns (22)–(24).

4. VARIATIONAL FORMULATION

For the purposes of developing element matrices it is useful to construct a variational functional the extremum conditions of which would yield the equilibrium equations derived above, and the related boundary conditions. This may be accomplished by writing the inner product of the equilibrium equations, when expressed in terms of the kinematic quantities, with the appropriate virtual displacements. It is useful to integrate such a virtual work expression by parts. Such an integration has the following desirable effects: (i) the associated boundary conditions become identified, (ii) the energy terms emerge, and (iii) derivatives of lower order will appear in the functional. The latter effect is of importance for interelement compatibility requirements. On carrying out this integration the following expressions for the strain energy and the virtual work of initial forces may be obtained:

$$\begin{aligned} U &= \frac{1}{2}\int_0^l \{\gamma GA\varepsilon_1^{*2} + \gamma GA\varepsilon_2^{*2} + EA\varepsilon_3^{*2} + EI_1k_1^{*2} + EI_2k_2^{*2} + GI_3k_3^{*2}\}\,\mathrm{d}s \\ &= \frac{1}{2}\int_0^l \{\gamma GA(u_1^{*\prime} - \tau u_2^* + \kappa u_3^* - \theta_2^*)^2 + \gamma GA(u_2^{*\prime} + \tau u_1^* + \theta_1^*)^2 \\ &\quad + EA(u_3^{*\prime} - \kappa u_1^*)^2 + EI_1(\theta_1^{*\prime} - \tau\theta_2^* + \kappa\theta_3^*)^2 \\ &\quad + EI_2(\theta_2^{*\prime} + \tau\theta_1^*)^2 + GI_3(\theta_3^{*\prime} - \kappa\theta_1^*)^2\}\,\mathrm{d}s, \end{aligned} \tag{31}$$

and

$$\begin{aligned} \delta W = \int_0^l \{ &-\tfrac{1}{2}Q_3\delta[(u_1^{*\prime} - \tau u_2^* + \kappa u_3^*)^2 + (u_2^{*\prime} + \tau u_1^*)^2] \\ &+ [Q_2\theta_3^*\delta(u_1^{*\prime} - \tau u_2^* + \kappa u_3^* - \theta_2^*) - Q_1\theta_3^*\delta(u_2^{*\prime} + \tau u_1^* + \theta_1^*)] \\ &+ [Q_1(u_1^{*\prime} - \tau u_2^* + \kappa u_3^*) + Q_2(u_2^{*\prime} + \tau u_1^*)]\delta(u_3^{*\prime} - \kappa u_1^*) \\ &+ [Q_1\theta_1^* + Q_2\theta_2^*]\delta\theta_3^* + [-M_3\theta_2^*\delta(\theta_1^{*\prime} - \tau\theta_2^* + \kappa\theta_3^*) \\ &+ M_3\theta_1^*\delta(\theta_2^{*\prime} + \tau\theta_1^*)] + [M_1\theta_2^* - M_2\theta_1^*]\delta(\theta_3^{*\prime} - \kappa\theta_1^*) \\ &+ [M_2\theta_3^*\delta(\theta_1^{*\prime} - \tau\theta_2^* + \kappa\theta_3^*) - M_1\theta_3^*\delta(\theta_2^{*\prime} + \tau\theta_1^*)]\}\,\mathrm{d}s. \end{aligned} \tag{32}$$

The terms in the round brackets, in the first term of this integral, are the slopes of the centreline. Hence the first term describes the work of the axial force Q_3 as it moves through a distance equal to the difference between the original length of the centreline (in the critical

state) and the projection of the centreline for the bent and twisted perturbed state, onto the centreline in the critical state. That is, this term is the generalization, to curved and twisted rods, of the familiar potential energy of the axial force for prismatic rods. Now while in the principal coordinates of the critical state the shear forces Q_1 and Q_2 have no components in the binormal and the normal directions, respectively, they will have components in the directions of the binormal and the normal of the perturbed state. These components, given by $Q_1\theta_3^*$ and $Q_2\theta_3^*$, will have virtual work contributions associated with the shear strains. These virtual work terms appear in the second term of the above integral. In a similar manner the components of Q_1 and Q_2 will have a virtual work term associated with the axial strain in the perturbed state. This work is given in the third term of the above integral. $Q_1\theta_1^*$ and $Q_2\theta_2^*$, in the fourth term, are the contributions of Q_1 and Q_2 to the torque per unit length and hence this term describes the virtual work by these incremental torques associated with the rotation θ_3^*. The fifth term accounts for the work of the components of twisting torque M_3, in the perturbed state, associated with changes of curvature in the normal and binormal directions. The sixth term takes account of the work done by the components of M_1 and M_2, in the perturbed state, associated with the changes of centreline rotation. Finally the seventh term accounts for the work of the components of M_1 and M_2, in the perturbed state, associated with changes of curvature in the normal and binormal directions.

With the energy terms at hand, one can write the expression for the virtual work theorem as

$$\delta\Pi - \delta U - \delta W. \tag{33}$$

By carrying out the variations and utilizing the equilibrium relations for the initial force quantities, one can show that

$$\begin{aligned}
\delta\Pi = \int_0^l \{ & \delta u_1^*[-\gamma GA(u_1^{*\prime} - \tau u_2^* + \kappa u_3^* - \theta_2^*)' + \tau\gamma GA(u_2^{*\prime} + \tau u_1^* + \theta_1^*) - \kappa EA(u_3^{*\prime} - \kappa u_1^*) \\
& + Q_2(\theta_3^{*\prime} + \kappa u_2^{*\prime} + \kappa\tau u_1^*) - Q_3(u_1^{*\prime\prime} - 2\tau u_2^{*\prime} + \kappa u_3^{*\prime} - \tau^2 u_1^*)] \\
& + \delta u_2^*[-\gamma GA(u_2^{*\prime} + \tau u_1^* + \theta_1^*)' - \tau\gamma GA(u_1^{*\prime} - \tau u_2^* + \kappa u_3^* - \theta_2^*) \\
& + Q_3(-u_2^{*\prime\prime} - 2\tau u_1^{*\prime} + \tau^2 u_2^* - \tau\kappa u_3^* + \kappa\theta_3^*) - Q_1(\theta_3^{*\prime} + \kappa u_2^{*\prime} + \kappa\tau u_1^*)] \\
& + \delta u_3^*[-EA(u_3^{*\prime} - \kappa u_1^*)' + \kappa\gamma GA(u_1^{*\prime} - \tau u_2^* + \kappa u_3^* - \theta_2^*) \\
& + Q_1(u_1^{*\prime\prime} - 2\tau u_2^{*\prime} + \kappa u_3^{*\prime} - \tau^2 u_1^*) - Q_2(-u_2^{*\prime\prime} - 2\tau u_1^{*\prime} + \tau^2 u_2^* - \tau\kappa u_3^* + \kappa\theta_3^*)] \\
& + \delta\theta_1^*[-EI_1(\theta_1^{*\prime} - \tau\theta_2^* + \kappa\theta_3^*)' + \tau EI_2(\theta_2^{*\prime} + \tau\theta_1^*) - \kappa GI_3(\theta_3^{*\prime} - \kappa\theta_1^*) \\
& + \tau\gamma GA(u_2^{*\prime} + \tau u_1^* + \theta_1^*) + M_2(\theta_3^{*\prime} - \kappa\theta_1^*) - M_3(\theta_2^{*\prime} + \tau\theta_1^*)] \\
& + \delta\theta_2^*[-EI_2(\theta_2^{*\prime} + \tau\theta_1^*)' - \tau EI_1(\theta_1^{*\prime} - \tau\theta_2^* + \kappa\theta_3^*) \\
& - \gamma GA(u_1^{*\prime} - \tau u_2^* + \kappa u_3^* - \theta_2^*) - M_1(\theta_3^{*\prime} - \kappa\theta_1^*) + M_3(\theta_1^{*\prime} - \tau\theta_2^* + \kappa\theta_3^*)] \\
& + \delta\theta_3^*[-GI_3(\theta_3^{*\prime} - \kappa\theta_1^*)' + \kappa EI_1(\theta_1^{*\prime} - \tau\theta_2^* + \kappa\theta_3^*) \\
& + M_1(\theta_2^{*\prime} + \tau\theta_1^*) - M_2(\theta_1^{*\prime} - \tau\theta_2^* + \kappa\theta_3^*)]\} \, \mathrm{d}s \\
& + \{\delta u_1^*[\gamma GA(u_1^{*\prime} - \tau u_2^* + \kappa u_3^* - \theta_2^*) + Q_3(u_1^{*\prime} - \tau u_2^{*\prime} + \kappa u_3^*) - Q_2\theta_3^*] \\
& + \delta u_2^*[\gamma GA(u_2^{*\prime} + \tau u_1^* + \theta_1^*) + Q_3(u_2^{*\prime} + \tau u_1^*) + Q_1\theta_3^*] \\
& + \delta u_3^*[EA(u_3^{*\prime} - \kappa u_1^*) - Q_1(u_1^{*\prime} - \tau u_2^* + \kappa u_3^*) - Q_2(u_2^{*\prime} + \tau u_1^*)] \\
& + \delta\theta_1^*[EI_1(\theta_1^{*\prime} - \tau\theta_2^* + \kappa\theta_3^*) + M_3\theta_2^* - M_2\theta_3^*] \\
& + \delta\theta_2^*[EI_2(\theta_2^{*\prime} + \tau\theta_1^*) - M_3\theta_1^* + M_1\theta_3^*] \\
& + \delta\theta_3^*[GI_3(\theta_3^{*\prime} - \kappa\theta_1^*) - M_1\theta_2^* + M_2\theta_1^*]\}|_0^l.
\end{aligned} \tag{34}$$

It is not difficult to see that the Euler–Lagrange equations that emerge from the above variations yield the correct equilibrium equations in translation and the correct boundary conditions, for incremental quantities. For equilibrium equations in rotation one finds that the curvature changes of the centreline namely κ^*, τ^* and $\kappa_\dagger^*$, which appear in the equilibrium equations (19)–(21), are replaced by the curvature changes associated with the constitutive relations, as given in eqns (28)–(30). This is not unexpected since in reality the moments and the twist act on finite size cross-sections and not on the centreline. For slender rods for which shear strains may be neglected the two forms of curvature change become identical as one can readily verify by solving for θ_2^* and $\theta_\dagger^*$ in eqns (25) and (26) and eliminating the same from eqns (28)–(30). The result found for changes of curvature will be identical to the expressions given in eqns (22)–(24).

5. A FINITE ELEMENT MODEL

With a variational statement at hand we are now in a position to develop a finite element model for the buckling analysis of spatial rods. Because of the ease with which polynomials are differentiated and integrated they are almost always used in the development of finite element models. However in some cases, such as that at hand, polynomials cannot describe the rigid body modes [see Tabarrok *et al.* (1988a)], and are therefore not suitable for the development of element matrices. Evidently exact solutions of the governing equations provide the best choice for the shape functions. For the problem at hand the exact solutions will be functions of the critical load and will result in a nonlinear eigenvalue system equation.

The solutions to the governing equations in the absence of initial (internal) and external forces provide a good compromise. This solution may be obtained from the equilibrium equations:

$$\{q\}' + [\chi]\{q\} = \{0\}, \tag{35}$$

and the constitutive relations

$$\{u^{*\prime}\} + [\chi]^{\mathrm{T}}\{u^*\} - [D]^{-1}\{q\} = \{0\}, \tag{36}$$

where $\{q\}^{\mathrm{T}} = [q_1\, q_2\, q_3\, m_1\, m_2\, m_3]$, $\{u^*\}^{\mathrm{T}} = [u_\dagger^*\, u_2^*\, u_3^*\, \theta_\dagger^*\, \theta_2^*\, \theta_3^*]$, and $[D]$ is a diagonal matrix containing the stiffness parameters γGA, γGA, EA, EI_1, EI_2 and GI_3 and

$$[\chi] = \begin{bmatrix} [c] & [0] \\ [J] & [c] \end{bmatrix}, \tag{37}$$

where

$$[c] = \begin{bmatrix} 0 & -\tau & \kappa \\ \tau & 0 & 0 \\ -\kappa & 0 & 0 \end{bmatrix}, \quad [J] = \begin{bmatrix} 0 & -1 & 0 \\ 1 & 0 & 0 \\ 0 & 0 & 0 \end{bmatrix}.$$

Because of the similarity of the form of these equations and that of the homogeneous linear equilibrium equations, the expressions for $\{q\}$ and $\{u^*\}$ have the same form as that given by Mottershead (1980). Use of these expressions will yield an exact stiffness matrix and an approximate geometric stiffness matrix in the system eigenvalue equation. Equations (35) and (36) are best solved by first obtaining a solution for $\{q\}$ from eqn (35) which upon substitution into eqn (36) will allow one to obtain a solution for $\{u^*\}$. Before doing so it is worth examining the form of the energy terms given in eqns (31) and (32). In terms of the above notation we may express U as

$$U = \frac{1}{2}\int_0^l (\{u^{*'}\} - [\chi]^T\{u^*\})^T[D](\{u^{*'}\} - [\chi]^T\{u^*\})\,ds. \tag{38}$$

Now using eqn (36) we may write this as:

$$U = \frac{1}{2}\int_0^l (\{q(s)\}^T[D]^{-1}\{q(s)\})\,ds. \tag{39}$$

Likewise the virtual work term may be expressed as:

$$\begin{aligned}\delta W = \int_0^l & -\frac{1}{2}Q_3\delta\left[\left(\frac{q_1(s)}{\gamma GA} + \theta_2^*\right)^2 + \left(\frac{q_2(s)}{\gamma GA} - \theta_1^*\right)^2\right] \\ & + \left[Q_2\theta_3^*\delta\left(\frac{q_1(s)}{\gamma GA}\right) - Q_1\theta_3^*\delta\left(\frac{q_2(s)}{\gamma GA}\right)\right] \\ & + \left[Q_1\left(\frac{q_1(s)}{\gamma GA} + \theta_2^*\right) + Q_2\left(\frac{q_2(s)}{\gamma GA} - \theta_1^*\right)\right]\delta\left(\frac{q_3(s)}{EA}\right) \\ & + (Q_1\theta_1^* + Q_2\theta_2^*)\delta\theta_3^* + \left[-M_3\theta_2^*\delta\left(\frac{m_1(s)}{EI_1}\right) + M_3\theta_1^*\delta\left(\frac{m_2(s)}{EI_2}\right)\right] \\ & + (M_1\theta_2^* - M_2\theta_1^*)\delta\left(\frac{m_3(s)}{GI_3}\right) + \left[M_2\theta_3^*\delta\left(\frac{m_1(s)}{EI_1}\right) - M_1\theta_3^*\delta\left(\frac{m_2(s)}{EI_2}\right)\right]ds.\end{aligned} \tag{40}$$

The functions to be integrated in eqns (39) and (40) appear as trigonometric and products of polynomials and trigonometric terms and they involve 12 integration constants. These constants may be related to six nodal variables (three in translation and three in rotation) at each end of the element. The transformation from the integration constants to the nodal variables may be incorporated into the integrations in eqns (39) and (40). That is, one may express the function $\{q(s)\}$ and $\{u^*(s)\}$ in terms of the nodal displacement variables $\{u^*\}_e$, i.e.

$$\{q(s)\} = [A(s)]\{u^*\}_e, \tag{41}$$

$$\{u^*(s)\} = [B(s)]\{u^*\}_e, \tag{42}$$

where $[A(s)]$ and $[B(s)]$ are the shape function matrices given in Mottershead (1980).

Then on using eqns (41) and (42) and employing six point Gaussian integrations, eqns (39) and (40) may be written, as:

$$U = \tfrac{1}{2}\{u^*\}_e^T[K]_e\{u^*\}_e, \tag{43}$$

$$\delta W = \lambda\{u^*\}_e^T[K_g]_e\delta\{u^*\}_e, \tag{44}$$

where λ is the stiffness load factor, and the stiffness matrix $[K]_e$ is symmetric while the geometric stiffness matrix $[K_g]_e$ is nonsymmetric; it may be symmetrized in the manner used by Ye and Gallagher (1983), i.e.

$$[K_g^s]_e = \tfrac{1}{2}([K_g]_e + [K_g]_e^T). \tag{45}$$

Following the conventional assembly procedure, the final system matrix eigenvalue equation is:

$$[K]\{u^*\} = \lambda[K_g^s]\{u^*\}. \tag{46}$$

6. IMPLEMENTATION

The finite element model developed here is based on the updated Lagrangian equilibrium equations, that is, the initial displacements are taken into account by updating the geometric configurations. More precisely eqn (46) may be written as:

$$[K(\kappa, \tau)]\{u^*\} = \lambda[K_g^s(\kappa, \tau)]\{u^*\}, \tag{47}$$

where κ, τ are curvature and twist, respectively, in the current state, as expressed in eqns (5) and (6). This element can thus be used in the buckling analysis of spatial rods of different configurations including the cases where the initial displacements have a significant effect on the rod's geometry, prior to buckling. For these cases, the solutions are obtained iteratively by solving eqn (47) and eqns (7) and (8). An effective procedure is as follows:

Step 1. In the initial undeformed state, when the load factor $P_0 = 0$, form the stiffness matrix $[K(\kappa_0, \tau_0)]$. Conduct a static analysis for a unit load and record $\{u(s)\}$, carry out the eigenvalue analysis with

$$[K(\kappa_0, \tau_0)]\{u^*\} = \lambda[K_g^s(\kappa_0, \tau_0)]\{u^*\}, \tag{48}$$

and find an estimate for λ and the mode $\{u^*\}$. In this case λ is the (linear) Euler buckling load;

Step 2. Consider a small incremental $\Delta P \leqslant \lambda$, and calculate the incremental changes in curvature, $\Delta\kappa$, and twist, $\Delta\tau$. If the prebuckled deformations are assumed small,†

$$\Delta\kappa = \Delta P(u_1'' - 2\tau_0 u_2' + \kappa_0 u_3' - \tau_0^2 u_1), \tag{49}$$

$$\Delta\tau = \Delta P(\theta_3' + \kappa_0 u_2' + \kappa_0\tau_0 u_1), \tag{50}$$

where the displacements correspond to the unit load, in Step 1. Now increase the load factor to $P_1 = P_0 + \Delta P$, then the curvature κ and twist τ for the current state become

$$\kappa = \kappa_0 + \Delta\kappa, \quad \tau = \tau_0 + \Delta\tau; \tag{51}$$

Step 3. Form $[K(\kappa, \tau)]$ and $[K_g^s(\kappa, \tau)]$, and carry out an eigenvalue analysis with

$$[K(\kappa, \tau)]\{u^*\} = (P_0 + \lambda)[K_g^s(\kappa, \tau)]\{u^*\}. \tag{52}$$

In this step λ is the incremental eigenvalue;

Step 4. Check for convergence. If λ is smaller than a preset tolerance value, stop, otherwise repeat Steps 2 and 3, with κ_0, τ_0 and P_0 replaced by the curvature, twist and current load factor obtained in the previous cycle of iteration.

For some spatial rods, such as pretwisted rods and deep arches for instance, which do not suffer significant prebuckling deformations, one does not need to distinguish between the configuration of undeformed state and that for the current deformed state. In these cases the first step in the above procedure will provide the final results, that is, the value of λ in eqn (49) will be the buckling load P_{cr}.

† In general $\Delta\kappa_1 \neq 0$. However for relatively small deformations $\Delta\kappa_1 \ll \Delta\kappa$. Thus one can assume that the principal directions of the cross-section coincide with the updated directions of the normal and the binormal to the centre line.

7. ILLUSTRATIVE EXAMPLES

As a first example consider the buckling of a set of helical springs. The dimensions of these springs with various L/D ratios are given in Table 1. Two types of boundary conditions are considered: (a) the springs are clamped at one end and at the other end only the rotations are set equal to zero, and (b) the springs are clamped at both ends except for the axial deflections at the upper ends. Results obtained by the iterative procedure, using two elements for each coil of six springs, along with those obtained from Haringx formula [see Wahl (1963)], are shown in Table 2. It is seen that for springs with small pitch angles the present element yields close but slightly lower buckling loads compared with Haringx theory. In the Haringx theory the effect of large pitch angles is not considered, i.e. the theory holds for small pitch angles only. This can be seen more clearly from the results for spring Nos 3 and 7 which have larger pitch angles. Spring Nos 1 and 2 with the second boundary conditions do not have buckling forms according to Haringx theory, and indeed there were no convergent solutions obtained by the present element. The results for the iterative process of spring No. 1 with 12 elements are shown in Table 3. With good linear characteristics, the springs were assumed to deform linearly in the prebuckled states. Therefore the incremental load ΔP for each iteration step was set equal to the actual

Table 1. Geometric sizes of springs (mm)

Spring No.	Length	Spring diameter	Wire diameter	No. of coils
1	100	25	5	6
2	50	10	2	10
3	240	40	8	6
4	720	100	25	15
5	90	10	4	15
6	120	10	2	20
7	240	20	4	6

Table 2. Critical loads for springs

Spring No.	L/D	Pitch angle (degree)	Critical loads (N) B.C. 1 F.E.M.	B.C. 1 Haringx†	B.C. 2 F.E.M.	B.C. 2 Haringx
1	4	11.98	1313.3	1336.5		
2	5	9.04	96.50	97.32		
3	6	17.7	2024.2	2108.1	10116.8	10771.8
4	7.2	8.69	10466.5	10545.7	48182.9	48329.6
5	9	10.8	539.6	545.76	2345.3	2356.0
6	12	10.8	18.75	19.00	77.95	79.05
7	12	32.5	221.4	253.3	906.9	1054.1

† The authors are indebted to one of the reviewers for pointing out the paper by Kruzelecki and Sychowski (1990) and computing the following results for these seven springs, by the method presented in this reference: 1303.5, 96.1, 2027.0, 10449.7, 537.5, 18.72, 221.4.

Table 3. Iterative process for spring No. 1 (12 elements)

Iterative No.	P	κ	τ	Δp
1	0	76.5527	16.2449	1084.4
2	1084.4	77.1241	13.5523	182.22
3	1266.6	77.2049	13.0922	36.934
4	1303.5	77.2208	12.9987	7.7494
5	1311.3	77.2241	12.9790	1.6376
6	1312.9	77.2248	12.9749	0.3466

Table 4. Convergence of buckling loads for spring No. 1

Buckling mode	Number of elements 6	8	10	12	18	24
1	1317.1	1315.8	1313.5	1313.3	1313.2	1313.0
2	1324.6	1322.3	1320.4	1320.3	1320.1	1319.9
3	4380.0	4358.5	4339.2	4340.0	4335.9	4334.7
4	4445.6	4369.5	4356.7	4348.8	4346.7	4345.4
5	8302.0	8169.1	8096.7	8070.8	8058.2	8052.8
6	8670.6	8189.9	8104.9	8083.8	8060.4	8054.9
7	12931.6	12249.7	12045.9	12006.6	11924.1	11909.7
8	13677.3	12432.6	12182.4	12067.0	12035.8	12020.4

incremental of the minimum eigenvalue (see Table 3). Table 4 shows the convergence of the buckling loads of spring No. 1 as the number of elements increases. It is seen that for the first buckling mode a very small number of elements, as few as one element per coil, yields results quite close to the converged values, and the use of two elements per coil yields results sufficiently accurate for higher order modes.

As a second example the buckling of a quarter-circular arch, with circular cross-section, was analysed under uniform external pressure. The two ends were pinned and the rotation about the centreline was set to zero. In order to show the full capability of the present element, both the in-plane and out-of-plane buckling analysis of the arch under both dead load and follower forces was carried out. In the latter case, with follower forces, the simple symmetrization of eqn (3) was not used in view of the nonconservative form of the follower force. The data used for this example are as follows:

$$E = 0.21 \times 10^{12}\ \text{Pa}, \quad \nu = 0.3, \quad R = 10\ \text{m}, \quad r = 0.1\ \text{m},$$

where R is the radius of the arch, and r the radius of the cross-section. Iterative computations show that the prebuckling deformations are not appreciable. Therefore only the first step of iteration was carried out and the buckling loads obtained for the two load cases are shown in Tables 5(a) and (b) respectively. It is seen that a small number of elements gives quite good results.

Table 5(a). Buckling loads of arch with dead load ($\times 10^5$ N)

Modes†	Number of elements 6	8	10	12	14	16	18	20	Analytical‡
1 (OPS)	0.2849	0.2828	0.2818	0.2813	0.2810	0.2808	0.2806	0.2805	0.2801
2 (OPA)	2.1960	2.1722	2.1617	2.1560	2.1527	2.1505	2.1490	2.1480	2.1451
3 (IPA)	2.6749	2.6473	2.6350	2.6284	2.6246	2.6221	2.6204	2.6192	2.6389
4 (OPS)	5.5738	5.4922	5.4586	5.4415	5.4316	5.4253	5.4211	5.4181	5.4167
5 (IPS)	6.0600	5.9774	5.9422	5.9243	5.9141	5.9076	5.9033	5.9003	5.8878

† OPS—out of plane, symmetric; OPA—out of plane, antisymmetric; IPA—in plane, antisymmetric; IPS—in plane, symmetric.

‡ Timoshenko (1961), Wempner (1973).

Table 5(b). Buckling loads of arch with follower force ($\times 10^5$ N)

Modes	Number of elements 6	8	10	12	14	16	18	20	Analytical†
1 (OPS)	0.5103	0.5034	0.5003	0.4986	0.4976	0.4970	0.4965	0.4962	0.4948
2 (OPA)	2.5406	2.5021	2.4911	2.4853	2.4818	2.4796	2.4781	2.4770	2.4740
3 (IPA)	2.5406	2.5095	2.4958	2.4884	2.4841	2.4813	2.4794	2.4780	2.4740
4 (IPS)	5.8736	5.8175	5.7751	5.7461	5.7365	5.7304	5.7263	5.7237	5.7229
5 (OPS)	5.9462	5.8559	5.8188	5.8000	5.7892	5.7823	5.7837	5.7744	5.7727

† Timoshenko (1961), Wempner (1973).

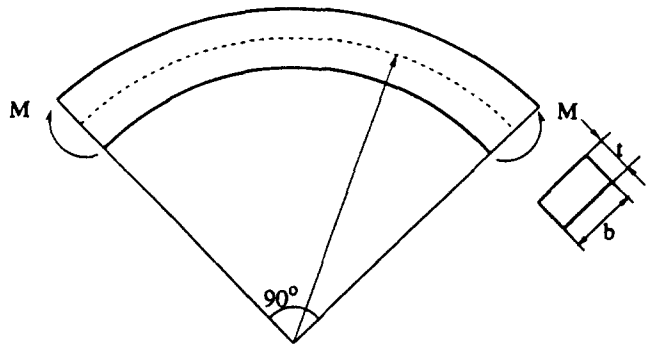

Fig. 3. A quarter circular arch with end couples.

As a final example the out-of-plane buckling of a quarter circular arch under terminal couples, as shown in Fig. 3, was analysed. This example cannot be analysed by means of an assemblage of prismatic beam elements, as found in most commercial FE programs since in such programs the effect of initial bending moments is neglected. The example data are as follows:

$$E = 0.21 \times 10^{12}\ \text{Pa}, \quad \nu = 0.3, \quad R = 10\ \text{m}, \quad b = 1.0\ \text{m}, \quad t = 0.05\ \text{m}.$$

Results obtained by the present element along with the analytical solution, are shown in Table 6, for the four lowest modes. It is seen that for the first buckling mode only two elements give quite good results.

Table 7 shows the results obtained by 12 elements for an arch subjected to end moments with various values of radius while the total length remains unchanged. It is seen that as the radius becomes larger, the first buckling load converges to the lateral buckling load of a thin straight beam (Timoshenko, 1961).

8. CONCLUDING COMMENTS

From the equilibrium equations of the perturbed state a variational function has been derived for the buckling analysis of spatially curved and twisted rods. Using this functional stiffness and geometric stiffness matrices have been derived for a general curved and twisted element.

The element takes account of initial bending moments and shear forces as well as the axial load. Furthermore the element can be used for buckling analysis of rods subjected to conservative and nonconservative follower type forces. Although the nonconservative problem analysed is of divergent type, formulation presented can be used for flutter type

Table 6. Buckling loads of an arch with end moments ($\times 10^5$ N)

Modes	Number of elements 2	4	6	8	10	12	14	16	Analytical†
1	0.2759	0.2701	0.2690	0.2687	0.2685	0.2684	0.2684	0.2683	0.2682
2	1.7393	0.8589	0.8312	0.8216	0.8171	0.8147	0.8133	0.8123	0.8093
3	4.4993	1.5572	1.4518	1.4079	1.3875	1.3764	1.3698	1.3655	1.3514
4	9.0722	7.2896	2.1552	2.0475	1.9925	1.9623	1.9441	1.9323	1.8938

† Timoshenko (1961), Wempner (1973).

Table 7. The first buckling load of arch with varying radius ($\times 10^6$ Nm)

R	10	20	100	200	500	1000	1250	
M_{cr}	0.2684	0.4053	0.5163	0.5302	0.5378	0.5417	0.5420	0.5427

nonconservative problems. In this case of course the kinetic criterion must be used and a mass matrix must be developed. This work is reported in a separate publication.

For some curved and twisted rods initial deformations become significant prior to buckling. The major contributions for such initial deformations come from finite rotations and result in changes in the rod's curvature and twist. A procedure has been outlined to incrementally account for such changes of geometry.

The illustrative examples given verify the formulation and demonstrate the rather good performance of the element developed.

REFERENCES

Abbas, B. A. H. (1979). Simple finite elements for dynamic analysis of thick pretwisted blades. *Aeronaut. Jl* **83**, 450–453.

Kruzelecki, J. and Syckowski, M. (1990). On the concept of an equivalent column in the stability problem of compressed helical springs. *Ing-Arch.* **60**, 367–377.

Mottershead, J. E. (1980). Finite elements for dynamical analysis of helical rods. *Int. J. Mech. Sci.* **22**, 267–283.

Mottershead, J. E. (1982). The large displacements and dynamic stability of springs using helical finite elements. *Int. J. Mech. Sci.* **24**, 547–558.

Tabarrok, B., Farshad, M. and Yi, H. (1988a). Finite element formulation of spatially curved and twisted rods. *Comp. Meth. Appl. Mech. Engng* **70**, 275–299.

Tabarrok, B., Sinclair, A. N., Farshad, M. and Yi, H. (1988b). On the dynamics of spatially curved and twisted rods—a finite element formulation. *J. Sound Vibr.* **123**, 315–326.

Tabarrok, B. and Xiong, Y. (1989). On the buckling equations of spatial rods. *Int. J. Mech. Sci.* **31**, 179–192.

Timoshenko, S. P. (1961). *Theory of Elastic Stability*. McGraw-Hill, New York.

Tomas, J. and Dokumaci, E. (1974). Simple finite elements for pretwisted blading vibration. *Aeronaut. Quart.* **25**, 109–118.

Wahl, A. M. (1963). *Mechanical Springs* (2nd edition). McGraw-Hill, New York.

Wempner, G. A. (1973). *Mechanics of Solids, with Applications to Thin Bodies*. McGraw-Hill, New York.

Xiong, Y. and Tabarrok, B. (1989). Buckling analysis of spatial rods by a new finite element model. *Recent Developments in Buckling of Structures*, ASME publication PVP-Vol. 183.

Yamada, Y. and Ezawa, Y. (1977). On curved finite element for the analysis of circular arches. *Int. J. Num. Meth. Engng* **11**, 1635–1651.

Ye, T. Q. and Gallagher, R. H. (1983). Instability analysis of pressure-loaded thin arches of arbitrary shape. *J. Appl. Mech.* **50**, 315–320.

APPENDIX

For the rod with follower distributed loads, an extra virtual work term, accounting for the contributions of the follower forces, must be appended to the functional. This term may be written as follows:

$$\delta W_d = \int_0^l \{p_1[\theta_3^*\delta u_2^* - (u_1^{*\prime} - \tau u_2^* + \kappa u_3^*)\delta u_3^*] + p_2[-\theta_3^*\delta u_1^* - (u_2^{*\prime} + \tau u_1^*)\delta u_3^*] + p_3[(u_1^{*\prime} - \tau u_2^* + \kappa u_3^*)\delta u_1^* + (u_2^{*\prime} + \tau u_1^*)\delta u_2^*] + t_1[\theta_3^*\delta\theta_2^* - \theta_2^*\delta\theta_3^*] + t_2[\theta_1^*\delta\theta_3^* - \theta_3^*\delta\theta_1^*] + t_3[\theta_2^*\delta\theta_1^* - \theta_1^*\delta\theta_2^*]\}\,ds, \quad \text{(A1)}$$

where $p_1, p_2, p_3, t_1, t_2, t_3$ are the distributed force and moment parameters. The various terms in the above integral may be interpreted in a manner similar to that used in eqn (32).